W-band EPR studies of high-spin nitrenes with large spin-orbit contribution to zero-field splitting

ARTICLE *in* THE JOURNAL OF CHEMICAL PHYSICS · AUGUST 2015

Impact Factor: 2.95 · DOI: 10.1063/1.4929589

6 AUTHORS, INCLUDING:

Aleksandr Akimov
Russian Academy of Sciences
7 PUBLICATIONS **4** CITATIONS
SEE PROFILE

Denis V. Korchagin
Russian Academy of Sciences
45 PUBLICATIONS **146** CITATIONS
SEE PROFILE

Sergei Victorovich Chapyshev
Russian Academy of Sciences
119 PUBLICATIONS **834** CITATIONS
SEE PROFILE

Eugenii Ya Misochko
Russian Academy of Sciences
65 PUBLICATIONS **522** CITATIONS
SEE PROFILE

W-band EPR studies of high-spin nitrenes with large spin-orbit contribution to zero-field splitting

Alexander Akimov,[1] Artem Masitov,[1] Denis Korchagin,[1] Sergei Chapyshev,[1] Eugenii Misochko,[1,a)] and Anton Savitsky[2]
[1]*Institute of Problems of Chemical Physics RAS, Chernogolovka, Russia*
[2]*Max-Planck Institute for Chemical Energy Conversion, Mulheim/Ruhr, Germany*

(Received 9 July 2015; accepted 14 August 2015; published online 28 August 2015)

First W-band 94 GHz EPR spectra of randomly oriented triplet, quintet, and septet nitrenes formed during the photolysis of 1,3,5-triazido-2,4,6-tribromobenzene in cryogenic matrices are reported. In comparison with conventional X-band 9 GHz electron paramagnetic resonance (EPR) spectroscopy, W-band EPR spectroscopy allows the detection and complete spectroscopic characterization of all paramagnetic species formed at different stages of the photolysis of aromatic polyazides. This type of spectroscopy is of paramount importance for experimental determination of the sign of the zero-field splitting (ZFS) parameters of high-spin molecules with large spin-orbit contribution to the ZFS, caused by the effect of heavy atoms. The study shows that triplet 1,3-diazido-2,4,6-tribromo-5-nitrenobenzene (**T1**) has D_T = 1.369 cm^{-1}, E_T = 0.093 cm^{-1}, and g = 2.0033, quintet 1-azido-2,4,6-tribromo-3,5-dinitrenobenzene (**Q1**) shows D_Q = −0.306 cm^{-1}, E_Q = 0.0137 cm^{-1}, and g = 2.0070, and septet 2,4,6-tribromo-1,3,5-trinitrenobenzene (**S1**) has D_S = −0.203 cm^{-1}, E_S = 0, and g = 2.0073. The experimental ZFS parameters agree well with the results of density functional theory calculations at the PBE/Ahlrichs-DZ level of theory, showing that such calculations adequately describe the magnetic properties of bromine-containing high-spin nitrenes. Both experimental and theoretical data indicate that, in contrast to all known to date quintet dinitrenes, dinitrene **Q1** has the negative sign of magnetic anisotropy due to the "heavy atom effect." This dinitrene along with septet trinitrene **S1** possess the largest negative value of D among all known quintet and septet organic polyradicals. © *2015 AIP Publishing LLC.* [http://dx.doi.org/10.1063/1.4929589]

I. INTRODUCTION

The first electron paramagnetic resonance (EPR) spectra of quintet and septet nitrenes, stabilized in frozen organic solutions, were reported for more than 40 yr ago.[1,2] Since then, large variety of polyradicals of this type were investigated by X-band EPR spectroscopy both in frozen organic solutions and in solid rare gas matrices. These studies showed that high-spin nitrenes have the largest zero-field splitting (ZFS) parameters $|D|$ among all organic polyradicals and are, thus, of considerable interest as model systems for studying magnetic anisotropy in organic molecules.[3–5] Some of high-spin nitrenes studied recently are shown in Scheme 1.

Extensive experimental and theoretical studies have shown that the dominant contribution to the ZFS parameter D of high-spin nitrenes arises from the dipolar spin-spin interaction between two unpaired electrons on the nitrene units.[6] Experimental ZFS parameters of such nitrenes can be well described with a semiempirical model[7] considering the ZFS tensor as a function of interactions between triplet nitrene units. In particular, this model predicts negative sign of D for molecules with three nitrene units (total spin S = 3) and positive sign of D for molecules with two nitrene units (total spin S = 2). Very recently, density functional theory (DFT)[6(i)] and *ab initio*[6(j)] calculations became available to calculate the ZFS in high-spin nitrenes. The calculations on containing light atoms nitrenes **1**-**4**, **6**, **7**, and **9**-**14** confirmed the dominant contribution of the dipolar spin-spin interactions (D_{SS}) to ZFS and showed that contributions of the anisotropic spin-orbit coupling (SOC) to the total parameter D of these nitrenes are relatively small (<10%). In our recent work, we have reported first high-spin nitrenes with dominant SOC contributions and unprecedentedly large magnitudes of $|D|$ owing to the effect of heavy bromine atoms (see trinitrene **5** and dinitrene **15** in Scheme 1).[8] Meanwhile, attempts to calculate the sign of the D_{SOC} and D values for **5** led to inconsistent results. According to our DFT calculations,[8] this trinitrene should have positive both D_{SOC} and D, while hybrid CASSCF-MRMP2 calculations predict negative D_{SOC} for **5**.[9] Again, different signs of D_{SOC} were predicted by DFT and CASSCF calculations for bromine-containing trinitrene **8**.[6(n)] These theoretical studies showed that conclusions about the sign of D for bromine-containing nitrenes strongly depend on the method of calculations. On the other side, the experimental data obtained by using conventional X-band (9.5 GHz) EPR spectroscopy also do not provide reliable information about the sign of D for high-spin organic molecules. The change in the sign of D in the standard magnetic spin Hamiltonian,

$$H = g\beta \mathrm{HS} + DS_z^2 + E\left(S_x^2 - S_y^2\right), \quad (1)$$

leads only to inversion of the Zeeman energy levels without changing the resonance fields of EPR transitions. Therefore,

a)Electronic mail: misochko@icp.ac.ru.

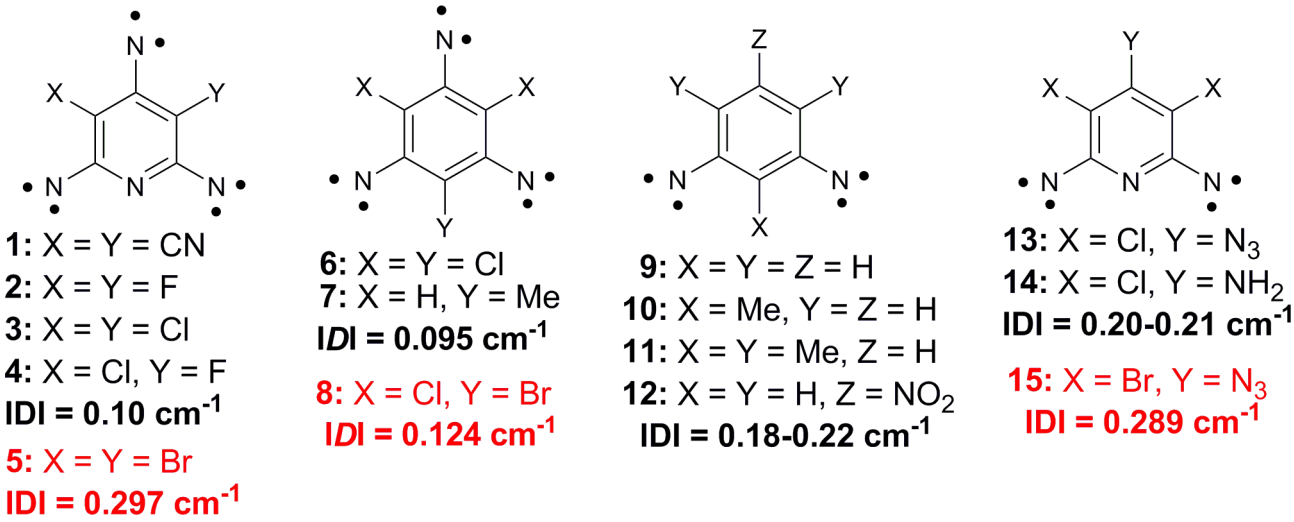

SCHEME 1. Some septet and quintet polynitrenes studied previously.

the sign of the parameter D can be derived from EPR spectra having a significant difference in the thermal populations between upper and lower Zeeman levels, i.e., the Zeeman temperature, $T_z = h\nu_0$, is comparable to the thermal energy kT.[10] Fortunately, the sign of D for high-spin molecular systems can experimentally be determined by using high field (high frequency) EPR spectroscopy at liquid helium temperature. For instance, the sign of D can reliably obtained from single EPR W-band (94 GHz, $T_Z = 4.5$ K) spectrum recorded at 5 K.[11] Thus, Q-band 34 GHz and W-band 94 GHz EPR spectroscopies are widely used for such purposes in studies of high-spin polynuclear transition metal complexes.[12] Recently, Q-band 34 GHz EPR spectroscopy was for the first time used to investigate quartet nitrenoradicals in cryogenic matrices.[13]

In the present work, we report on the first-ever recorded W-band EPR spectra of triplet, quintet, and septet nitrenes. These spectra were recorded for new triplet mononitrene **T1**, quintet dinitrene **Q1**, and septet trinitrene **S1** obtained by the photolysis of triazide **TA** in cryogenic matrices (Scheme 2). The choice of **T1**, **Q1**, and **S1** as model systems was dictated by the results of recent theoretical studies[8] predicting the large negative value of D for trinitrene **S1**.

The main goal of the work was the detection and analysis of the W-band EPR spectra of **T1**, **Q1**, and **S1**, including determination of the signs and magnitudes of the D and E values for these species. To evaluate the performance of various experimental and theoretical approaches to investigation of multicomponent multispin molecular systems, nitrenes **T1**, **Q1**, and **S1** were studied as well by using conventional X-band EPR spectroscopy and modern DFT calculations.

II. EXPERIMENTAL SECTION

A. Starting materials

Triazide **TA** was synthesized according to a literature procedure.[14] The solvent methylcyclohexane (MCH) was obtained from Sigma-Aldrich in their purest commercially available form and used without further purification.

B. EPR measurements

X-band cw EPR spectra of high spin nitrenes were recorded after the photolysis of triazide **TA** in solid argon matrix and in methylcyclohexane glass. Experimental technique for the matrix isolation used in this study was similar to that described earlier.[8] Solid argon films doped with triazide **TA** were prepared by vacuum co-deposition of two separate molecular beams (Ar and triazide **TA** vapor) onto a substrate (sapphire rod) cooled to 15 K. The deposition rate was typically 10 μmol/min; the thickness of the deposited argon films was typically 100 μm. The vapor of **TA** was produced with oven heating of the polycrystalline **TA** to ca 104 °C. The oven temperature was regulated by a precise temperature controller and was chosen to obtain the ratio of Ar/triazide **TA** ~10^3–10^4. Temperature stability was ~0.1 K over 15–40 K range. EPR spectra were recorded using a standard 9 GHz spectrometer at sufficiently low microwave power to avoid the saturation effects. Photolysis of the samples was carried out at temperature 15 K by means of a Hg arc lamp (Mercury Spectral Line Lamp, Lot-Oriel) equipped with narrow band filter transparent 297 nm. Additional X-band EPR measurements were performed in glassy MCH. In a typical procedure, triazide

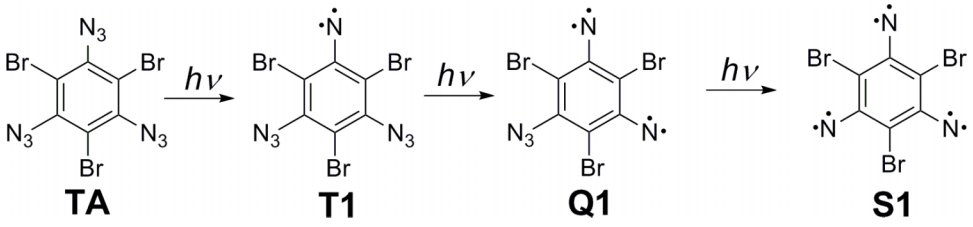

SCHEME 2. Photochemical generation of nitrenes **T1**, **Q1**, and **S1**.

TA was dissolved in freshly distilled MCH with the ratio of TA:MCH = 1:1000, placed in a 5 mm o.d. quartz EPR tube, subjected to 5-fold freeze-pump-thaw procedure, and the tube was sealed under vacuum. The sample tube was placed in the cavity of EPR spectrometer equipped with helium gas-flow thermostat. Then, the sample was cooled to 15 K to form a glass and photolyzed by means of a Hg arc lamp.

The pulsed EPR experiments were performed on a modified commercial W-band EPR spectrometer (Bruker Elexsys E680) operating at about 94 GHz.[15] The deoxygenated sample solutions were placed in a quartz capillary (0.6 mm I.D.) and transferred to the precooled EPR probehead. The samples were illuminated at 5 K using a Hg arc lamp guided to the sample through a quartz fiber of 0.4 mm diameter. The field-swept echo-detected EPR spectra were acquired at 5 K using the Hahn-echo sequence (t_p)-τ-$(2t_p)$-τ-echo with t_p = 20 ns and interpulse distance of τ = 180 ns. At each field point, 1024 echo responses were averaged after subsequent pulse sequences repeated 8×10^3 times per second.

C. DFT calculations

The geometries of the molecules were optimized at B3LYP/TZVP level of theory by DFT method. The nature of the stationary points was assessed by means of vibrational frequency analysis. The ZFS parameters were obtained from additional single-point calculations by using for this purpose the unrestricted Kohn-Sham determinant with the Perdew-Burke-Ernzerhof (PBE) functional[16] and the Ahlrichs-DZ basis set.[17] Calculations of the direct spin-spin coupling (D_{SS}) and spin-orbit coupling (D_{SOC}) parts of the ZFS parameters were performed by using the equation of McWeeny-Mizuno[18,19] and Pederson-Khanna approach,[20] respectively. The combination of these approaches and the PBE/Ahlrichs-DZ level of theory provided the most accurate data for high-spin nitrenes.[6(k),6(p),8] All calculations were performed with the ORCA program package (version 3.0.3).[21]

III. RESULTS AND DISCUSSION

A. X-band EPR spectra in solid argon and MCH

Short UV irradiation (15 min, λ = 297 nm) of triazide **TA**, isolated in solid argon matrix at 15 K, leads to the appearance of a series of EPR lines at 50, 81, 170, and 196 mT in the X-band cw EPR spectrum. Upon further irradiation, a number of additional weak EPR lines at 386, 407, 642, and 665 mT appeared in the spectrum. The intensities of the EPR lines reached their maximum after 50 min irradiation time and then gradually decayed on further irradiation. Since all observable EPR lines, except one at 50 mT, show the same kinetics, they can be assigned to the same paramagnetic product. The EPR line at 50 mT indicates on the formation of a second paramagnetic product. The final EPR spectrum recorded after 50 min irradiation time is shown in Fig. 1(a).

Prolonged irradiation (30 min, λ = 297 nm) of triazide **TA** in glassy MCH produced EPR spectrum, which practically reproduced the EPR spectrum in the solid argon matrix, see Fig. 1(c). As rule, the EPR lines in organic glass are broader

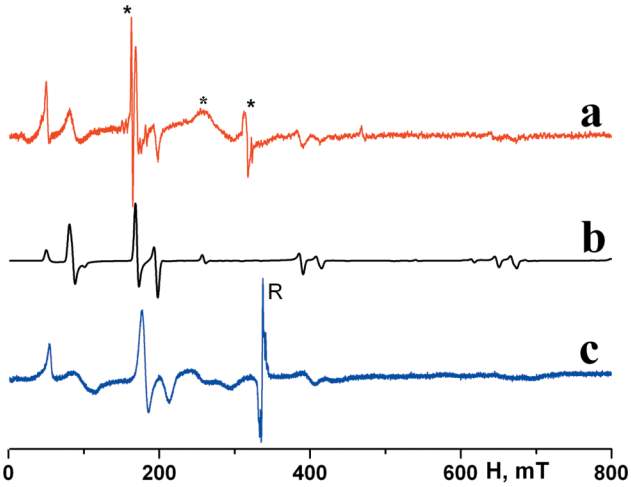

FIG. 1. X-band cw EPR spectra: (a) after UV irradiation of triazide TA in solid argon matrix at 15 K, microwave frequency 8.899 GHz; (b) simulation for trinitrene **S1** with $|D_S| = 0.202$ cm^{-1}, $E_S = 0$ and g = 2.0023. Microwave frequency 8.899 GHz; (c) after UV irradiation of triazide **TA** in glassy MCH at 15 K, microwave frequency 9.4330 GHz; the EPR lines from the impurities in the sapphire rod are marked with (*). The EPR line from radical species formed in the organic matrix is marked as R.

compared to that recorded in argon matrices.[6(g)] The differences in the resonances of the strong EPR lines are due to different microwave frequencies for the measurements in solid argon and MCH glass. Additionally, the structureless EPR line at 330 mT appears in glassy MCH, which is assigned to radical species formed due to photolytic reactions in the organic matrix.

According to previous studies,[8] the strongest lines in the X-band EPR spectra of products formed during the photolysis of 1,3,5-triazidobenzenes arise from septet trinitrenes. Therefore, we started to analyze our experimental spectra from the line-shape EPR spectral simulations for trinitrene **S1.** The spectral simulations were performed using the *EasySpin* program package,[22] operating with an exact numerical matrix diagonalization of spin Hamiltonian (1) for randomly oriented molecules with total spin S = 3. The ZFS parameters of trinitrene **S1** were determined by comparison of the computer simulated and experimentally recorded spectra. This procedure was described in detail in Refs. 6(d) and 8. Three intense EPR lines at 81, 170, and 196 mT in the experimental spectrum were used as the references. The best agreement between experimental and simulated spectra was achieved for $|D_S| = 0.202$ cm^{-1}, $E_S = 0$, and g = 2.0023. Fig. 1(b) demonstrates that all intense EPR lines in the calculated spectrum reproduce intense EPR lines in the experimental spectrum. To estimate an accuracy of $|D_S|$ and E_S measurements, the EPR spectra were calculated by varying each of the parameters nearby their optimum values. The deviation was chosen as crucial one, if at least one of the tested lines had deviation $|H_{calc}–H_{exp}|$ exceeding the line width. This treatment gave the experimental errors for $|D_S|$ and E_S not more than ±0.001 and ±0.0005 cm^{-1}, respectively. The calculated spectrum reproduces as well a series of weak EPR lines at 50, 386, 407, 642, and 665 mT observed in the experiment. It is interesting to note that intensity of the low-field EPR line at 50 mT in the calculated spectrum is much lower as compared to experimental one. Most probably, the

high intensity of this line in the experimental spectra is due to its superposition with an intense line of quintet dinitrene **Q1**. This also explains the different kinetic behaviors observed at 50 mT during the photolysis of **TA**. Thus, we conclude that experimental spectra in Fig. 1 are almost pure X-band EPR spectra of septet trinitrene **S1**. Assignment of all lines in the powder X-band EPR spectrum of **S1** is shown in the supplementary material.[23] The $|D_S|$ value of this trinitrene exceeds twice the $|D_S|$ values of other septet trinitrenes containing light atoms in the molecules (see Scheme 1). At the same time, $|D_S| = 0.202\ cm^{-1}$, derived from the experimental EPR spectra, lies close to $D = -0.24\ cm^{-1}$ that was recently predicted for **S1** by DFT calculations.[8]

B. W-band EPR spectrum in glassy MCH

Figure 2 shows the final W-band EPR spectrum recorded after photolysis of **TA** in glassy MCH at 5 K. It reveals a series of intense lines in the region of free electron g-factor, g_e. The EPR spectrum is spread over about 2 T, having the low-field border at 2250 mT and the high-field border at 4000 mT. The calculated spectrum for trinitrene **S1** with $D_S = -0.202\ cm^{-1}$ and $E_S = 0$ (blue line 2 in Fig. 2) coincides with several strong peaks in the experimental spectrum (labeled as S in Fig. 2). A precise fitting procedure yields $D_S = -0.203 \pm 0.001\ cm^{-1}$, $E_S = 0$, and g = 2.0073 for trinitrene **S1**. It is especially important to note that a good agreement between intensities of the peaks in the experimental and theoretical spectra of **S1** is observed only when the parameter D_S is negative. Considerable differences between the W-band EPR spectra of **S1** with the positive sign and negative sign of D_S, confirming the negative sign of D_S for **S1,** are illustrated in Fig. 3(a).

A series of other spectral features in the experimental spectrum (labeled as Q in Fig. 2) is assigned to quintet dinitrene

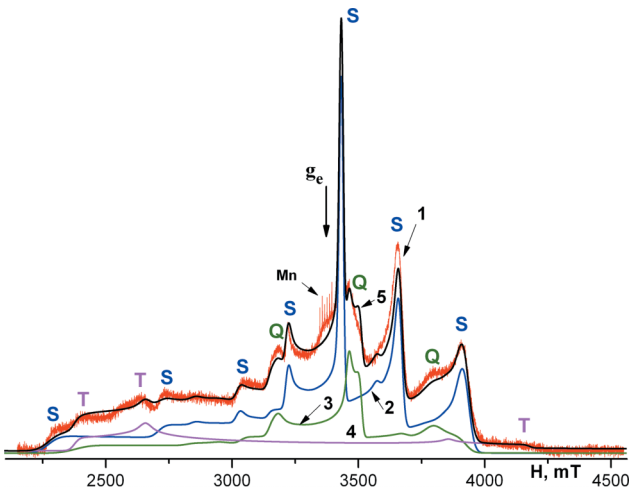

FIG. 2. W-band field-swept echo-detected absorption EPR spectrum at temperature 5 K: 1 (red line)—after UV irradiation of triazide **TA** in glassy MCH; 2 (blue line)—simulation for trinitrene **S1** with $D_S = -0.203\ cm^{-1}$, $E_S = 0$ and g = 2.0073; 3 (green line)—simulation for quintet dinitrene **Q1** with $|D_Q| = 0.302\ cm^{-1}$, $E_Q = 0.0137\ cm^{-1}$ and g = 2.0070; 4 (violet line)—simulation for triplet mononitrene **T1** with $D_T = 1.369\ cm^{-1}$, $E_T = 0.093\ cm^{-1}$, and g = 2.0033; 5 (dark line)—simulation for **T1**, **Q1**, and **S1** in the ratio 1:0.4:0.6, respectively. Abbreviations S, Q, and T show the EPR transitions in trinitrene **S1,** dinitrene **Q1,** and mononitrene **T1**, respectively. Microwave frequency 93.997 GHz.

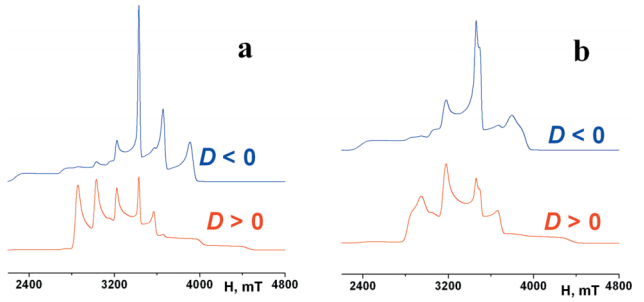

FIG. 3. Calculated W-band absorption EPR spectra of septet trinitrene with $|D_S| = 0.203\ cm^{-1}$, $E_S = 0$, and g = 2.0073 (a) and quintet dinitrene with $|D_Q| = 0.302\ cm^{-1}$, $E_Q = 0.0137\ cm^{-1}$, and g = 2.0070 (b). Temperature 5 K. Microwave frequency 93.997 GHz.

Q1. The line-shape spectral simulations for this dinitrene with total spin S = 2 give the best fit to the experimental spectrum for $D_Q = -0.306 \pm 0.001\ cm^{-1}$, $E_Q = 0.0137 \pm 0.0005\ cm^{-1}$, and g = 2.0070 (green line 3 in Fig. 2). The line-shape spectral simulations of the W-band EPR spectra of **Q1** with the positive sign and negative sign of D_Q confirm that this dinitrene has the negative D_Q, see Fig. 3(b). Thus, this is the first time when a quintet dinitrene with negative sign of D_Q was observed. The remaining weak lines in the experimental spectrum (labeled as T) allowed us to determine the ZFS parameters of triplet nitrene **T1** as $D_T = 1.369 \pm 0.002\ cm^{-1}$ and $E_T = 0.093 \pm 0.001\ cm^{-1}$.

Thus, the experimental W-band EPR spectrum in Fig. 2 represents a sum of spectra of triplet nitrene **T1**, quintet dinitrene **Q1**, and septet trinitrene **S1**. The computer simulation of this spectrum for **T1**/**Q1**/**S1** = 1/0.4/0.6 is shown in Fig. 2 (dark line 5). The spectra of these three nitrenes completely describe all experimental features. The ZFS parameters of trinitrene **S1** derived from the X-band and W-band EPR spectra are identical, while the experimental spectra of dinitrene **Q1** and mononitrene **T1** cannot not be detected by conventional X-band EPR spectroscopy due to its much lower cw EPR intensity.

C. DFT calculations

The $\hat{D}_{SS}$ tensors of spin-spin contributions and the $\hat{D}_{SOC}$ tensors of spin-orbit couplings for nitrenes **T1**, **Q1**, and **S1** were calculated separately. The total ZFS tensor $\hat{D}_{Tot}$ was obtained by summing $\hat{D}_{SS}$ and $\hat{D}_{SOC}$. The ZFS parameters D_{SS}, D_{SOC}, and D_{Tot} were calculated by diagonalization of the tensors $\hat{D}_{SS}$, $\hat{D}_{SOC}$, and $\hat{D}_{Tot}$, respectively. The scalar ZFS parameters D and E were calculated with conventional notations,

$$D = \frac{3}{2}D_{zz}, \quad E = \frac{D_{xx} - D_{yy}}{2}, \tag{2}$$

where D_{xx}, D_{yy}, and D_{zz} are the eigenvalues of the tensor $\hat{D}$. The results of DFT calculations are given in Table I.

In accordance with our previous DFT calculations,[8] the tensors $\hat{D}_{SS}$ and $\hat{D}_{SOC}$ coincide, and the "easy axis" Z is perpendicular to the molecular plane of the D_{3h} symmetric septet trinitrene **S1**. Therefore, the total D value becomes the scalar sum of the SS and the SOC contributions, $D_{Tot} = D_{SS} + D_{SOC}$. The calculations predict the negative sign of both D_{SS}

TABLE I. Experimental and theoretical parameters D and E(cm^{-1}) of nitrenes **T1**, **Q1**, and **S1**.

Molecule	D_{SS}	D_{SOC}	D_{Tot}	D (Expt.)	E_{SS}	E_{SOC}	E_{Tot}	E (Expt.)
T1	0.992	0.421	1.413	1.3692	0.005	0.076	0.081	0.0932
Q1	0.196	0.212	−0.331	−0.3062	0.037	0.048	−0.003	0.0137
S1	−0.093	−0.147	−0.240	−0.2032	0.000	0.000	0.000	0.0000

and D_{SOC}. Subsequently, the total parameter D_{Tot} is predicted to be negative, in agreement with experimental data. The D_{SOC} contribution to D_{Tot} of **S1** is dominant and reaches 61%. Therefore, the parameter D_S of trinitrene **S1** exceeds twice the D_S values of trinitrenes **1-4** and **6-8**, for which the D_{SOC} parts are negligibly small.

Unexpectedly, the experimental W-band spectrum shows the negative sign of D_Q for dinitrene **Q1**, while all other known dinitrenes, including dibromine-containing dinitrene **15**, have positive parameters D_Q. Our DFT calculations also predict the negative sign of D_{Tot} for dinitrene **Q1** (Table I). In this dinitrene, the principal axes of the tensors $\hat{D}_{SS}$ and $\hat{D}_{SOC}$ have different orientations (Fig. 4). The Z-axis of the tensor $\hat{D}_{SS}$ coincides with the line connecting the nitrene units, while Z-axis of the tensor $\hat{D}_{SOC}$ is directed along the C–N bond of the azido group. Both parameters, D_{SS} and D_{SOC}, have positive signs and similar magnitudes. However, the Z-axis of the tensor $\hat{D}_{Tot}$ lies perpendicular to the molecular plane and has a negative sign. The diagonalization of the tensor $\hat{D}_{Tot}$ yields D_{Tot} = −0.331 cm^{-1}, which is in good agreement with D_Q = −0.306 cm^{-1} obtained experimentally. At the same time, DFT calculations notably underestimate the parameter E_{Tot} of **Q1** in comparison with the experimental value (Table I).

According to previous EPR studies and quantum-chemical calculations, typical D values of triplet phenyl nitrenes vary from 0.9 to 1.1 cm^{-1}, in which the contribution of the SOC term does not exceeds 10%.[24,4] Therefore, the experimental value of D_T = 1.369 cm^{-1} for nitrene **T1** is extraordinarily large. Indeed, DFT calculations predict a typical value of D_{SS} = 0.99 cm^{-1} for nitrene **T1**. Significant contribution to the total parameter D_{Tot} = 1.41 cm^{-1} arises due to the SOC term with contribution to D_{Tot} about 30%.

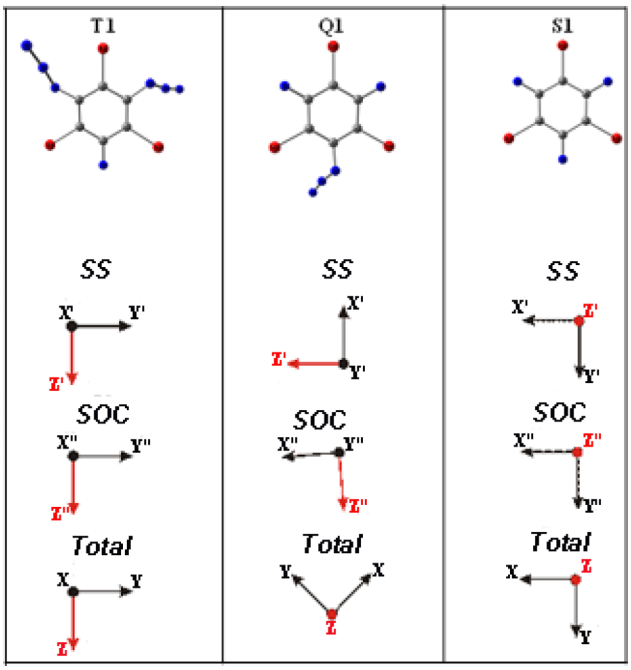

FIG. 4. The general view and the principal axes of $\hat{D}_{SS}$ (x′, y′, z′), $\hat{D}_{SOC}$ (x″, y″, z″), and $\hat{D}_{Tot}$ (x, y, z) tensors of nitrenes **T1**, **Q1**, and **S1**.

IV. CONCLUSIONS

The W-band EPR spectra of triplet, quintet, and septet nitrenes are manifested in the 2250–4250 mT region. From comparison with conventional X-band cw EPR spectroscopy, W-band EPR is more sensitive and allows to detect and characterize all paramagnetic products formed at different stages of aromatic polyazides photolysis. This type of spectroscopy is particularly helpful for determination of the sign of ZFS parameter D for high-spin molecules with large spin-orbit contribution to the ZFS, caused by the effect of heavy atoms. The present study shows that three new nitrenes, triplet nitrene **T1**, quintet dinitrene **Q1**, and septet trinitrene **S1**, are the paramagnetic products of the photolysis of triazide **TA**. Each of these nitrenes possesses unusual magnetic characteristics. Among triplet phenyl nitrenes, **T1** shows one of the highest values of D_T known up to now. In contrast to all reported quintet dinitrenes, **Q1** has the negative sign of D_Q. Moreover, its $|D_Q|$ is very large. Finally, trinitrene **S1** has the largest negative value of D_S among all septet trinitrenes. In the last case, the same value of $|D_S|$ for **S1** was derived from both the W-band and X-band EPR spectra. The experimental ZFS parameters of **T1**, **Q1,** and **S1** agree well with the results of DFT calculations, showing that such calculations adequately describe the magnetic properties of bromine-containing high-spin nitrenes. In overall, the combination of W-band EPR spectroscopy with conventional X-band EPR spectroscopy and modern DFT calculations is demonstrated to have numerous benefits of such an approach for investigation of randomly oriented multi-component multi-spin molecular systems possessing equally large spin-spin and spin-orbit interactions.

ACKNOWLEDGMENTS

This work was supported by the Russian Foundation for Basic Research (Grant No. 13-03-00757) and the Russian Academy of Sciences (Program No. OX-01), the Cluster of Excellence RESOLV (No. EXC 1069) funded by the Deutsche Forschungsgemeinschaft and the Max Planck Society.

[1]E. Wasserman, R. W. Murray, W. A. Yager, A. M. Trozzolo, and G. Smolinsky, J. Am. Chem. Soc. **89**, 5076 (1967).
[2]E. Wasserman, K. Schueller, and W. A. Yager, Chem. Phys. Lett. **2**, 259 (1968).

[3]K. Sugisaki, K. Toyota, K. Sato, D. Shiomi, M. Kitagawa, and T. Takui, in *EPR of Free Radicals in Solids I*, Progress in Theoretical Chemistry and Physics Vol. 24, edited by A. Lund and M. Shiotani (Springer Science and Business Media, Dordrecht, 2013), p. 363.
[4]D. Grote and W. Sander, in *Nitrene and Nitrenium Ions*, edited by D. E. Falvey and A. D. Gudmundsdottir (John Wiley & Sons, Inc., Hoboken, New Jersey, 2013), pp. 317–346.
[5]M. Baumgarter, in *EPR of Free Radicals in Solids II*, Progress in Theoretical Chemistry and Physics Vol. 25, edited by A. Lund and M. Shiotani (Springer Science and Business Media, Dordrecht, 2013), p. 205.
[6](a) S. V. Chapyshev, R. Walton, J. A. Sanborn, and P. M. Lahti, J. Am. Chem. Soc. **122**, 1580 (2000); (b) S. V. Chapyshev and H. Tomioka, Bull. Chem. Soc. Jpn. **76**, 2075 (2003); (c) S. V. Chapyshev, Russ. Chem. Bull. **55**, 1126 (2006); (d) S. V. Chapyshev, D. Grote, C. Finke, and W. Sander, J. Org. Chem. **73**, 7045 (2008); (e) E. Ya. Misochko, A. V. Akimov, and S. V. Chapyshev, J. Chem. Phys. **128**, 124504 (2008); (f) E. Ya. Misochko, A. V. Akimov, and S. V. Chapyshev, J. Chem. Phys. **129**, 174510 (2008); (g) S. V. Chapyshev, E. Ya. Misochko, A. V. Akimov, V. G. Dorokhov, P. Neuhaus, D. Grote, and W. Sander, J. Org. Chem. **74**, 7238 (2009); (h) T. Koto, K. Sato, D. Shiomi, K. Toyota, K. Itoh, E. Wasserman, and T. Takui, J. Phys. Chem. A **113**, 9521 (2009); (i) T. Koto, K. Sugisaki, K. Sato, D. Shiomi, K. Toyota, K. Itoh, E. Wassermann, P. M. Lahti, and T. Takui, Appl. Magn. Reson. **37**, 703 (2010); (j) S. V. Chapyshev, P. Neuhaus, D. Grote, and W. Sander, J. Phys. Org. Chem. **23**, 340 (2010); (k) E. Ya. Misochko, D. V. Korchagin, K. V. Bozhenko, S. V. Chapyshev, and S. M. Aldoshin, J. Chem. Phys. **133**, 064101 (2010); (l) K. Sugisaki, K. Toyota, K. Sato, D. Shiomi, M. Kitagawa, and T. Takui, ChemPhysChem **11**, 3146 (2010); (m) K. Sugisaki, K. Toyota, K. Sato, D. Shiomi, M. Kitagawa, and T. Takui, Phys. Chem. Chem. Phys. **13**, 6970 (2011); (n) E. Ya. Misochko, A. V. Akimov, A. A. Masitov, D. V. Korchagin, S. M. Aldoshin, and S. V. Chapyshev, J. Chem. Phys. **138**, 204317 (2013); (o) S. V. Chapyshev, D. V. Korchagin, P. Neuhaus, and W. Sander, Beilstein J. Org. Chem. **9**, 733 (2013); (p) E. Ya. Misochko, A. A. Masitov, A. V. Akimov, D. V. Korchagin, and S. V. Chapyshev, J. Phys. Chem. A **119**, 2413 (2015).
[7]K. Itoh, Pure Appl. Chem. **50**, 1251 (1978).
[8]E. Ya. Misochko, A. V. Akimov, A. A. Masitov, D. V. Korchagin, I. K. Yakushchenko, and S. V. Chapyshev, J. Chem. Phys. **137**, 064308 (2012).
[9]K. Sugisaki, K. Toyota, K. Sato, D. Shiomi, M. Kitagawa, and T. Takui, Phys. Chem. Chem. Phys. **16**, 9171 (2014).
[10]A. W. Hornig and J. S. Hyde, Mol. Phys. **6**, 33 (1963).
[11]S. D. Chemerisov, O. Y. Grinberg, D. S. Tipikin, Y. S. Lebedev, H. Kurreck, and K. Möbius, Chem. Phys. Lett. **218**, 353 (1994).
[12]A. Ozarowski, Inorg. Chem. **47**, 9760 (2008).
[13]T. L. Allen and P. M. Lahti, J. Phys. Chem. A **115**, 4922 (2011).
[14]S. V. Chapyshev and A. V. Chernyak, J. Fluorine Chem. **156**, 303 (2013).
[15]A. Nalepa, K. Möbius, W. Lubitz, and A. Savitsky, J. Magn. Reson. **242**, 203 (2014).
[16]J. P. Perdew, K. Burke, and M. Ernzerhof, Phys. Rev. Lett. **77**, 3865 (1996).
[17]A. Schafer, H. Horn, and R. Ahlrichs, J. Chem. Phys. **97**, 2571 (1992).
[18]R. McWeeny and Y. Mizuno, Proc. R. Soc. A **259**, 554 (1961).
[19]T. T. Petrenko, T. L. Petrenko, and V. Y. Bratus, J. Phys.: Condens. Matter **14**, 12433 (2002).
[20]M. R. Pederson and S. N. Khanna, Phys. Rev. B **60**, 9566 (1999).
[21]F. Neese, "The ORCA program system," Wiley Interdiscip. Rev.: Comput. Mol. Sci. **2**, 73 (2012).
[22]S. Stoll and A. Schweiger, J. Magn. Reson. **178**, 42 (2006).
[23]See supplementary material at http://dx.doi.org/10.1063/1.4929589 for (a) Zeeman energy levels and allowed X-band and W-band EPR transitions of septet trinitrene **S1**; (b) Zeeman energy levels and allowed W-band EPR transitions of quintet dinitrene **Q1**; (c) cartesian coordinates of nitrenes studied.
[24]D. Kvaskoff, P. Bednarek, L. George, K. Waich, and C. Wentrup, J. Org. Chem. **71**, 4049 (2006).